PSD-95 regulates synaptic kainate receptors at mouse hippocampal mossy fiber-CA3 synapses

Etsuko Suzuki[1, 2] and Haruyuki Kamiya[1]

[1]*Department of Neurobiology, Hokkaido University Graduate School of Medicine, Sapporo, 060-8638, Japan*

[2]*Japan Society for the Promotion of Science, Tokyo, 102-0083, Japan*

Corresponding author: Haruyuki Kamiya, M.D., Ph.D.

Department of Neurobiology, Hokkaido University Graduate School of Medicine, Sapporo, 060-8638, Japan

Phone: 81-11-706-5027 Fax 81-11-706-7863

E-mail: kamiya@med.hokudai.ac.jp

Total of number of pages; 37, Figures; 4, Tables; 0

Abstract

Kainate-type glutamate receptors (KARs) are the third class of ionotropic glutamate receptors whose activation leads to the unique roles in regulating synaptic transmission and circuit functions. In contrast to AMPA receptors (AMPARs), little is known about the mechanism of synaptic localization of KARs. PSD-95, a major scaffold protein of the postsynaptic density, is a candidate molecule that regulates the synaptic KARs. Although PSD-95 was shown to bind directly to KARs subunits, it has not been tested whether PSD-95 regulates synaptic KARs in intact synapses. Using PSD-95 knockout mice, we directly investigated the role of PSD-95 in the KARs-mediated components of synaptic transmission at hippocampal mossy fiber-CA3 synapse, one of the synapses with the highest density of KARs. Mossy fiber EPSCs consist of AMPA receptor (AMPAR)-mediated fast component and KAR-mediated slower component, and the ratio was significantly reduced in PSD-95 knockout mice. The size of KARs-mediated field EPSP reduced in comparison with the size of the fiber volley. Analysis of KARs-mediated miniature EPSCs also suggested reduced synaptic KARs. All the evidence supports critical roles of PSD-95 in regulating synaptic KARs.

Keywords: kainate receptor, postsynaptic density, PSD-95, hippocampus

1. Introduction

Excitatory synaptic transmission in the central nervous system is mostly mediated by AMPA-type glutamate receptors (AMPARs) and NMDA-type glutamate receptors (NMDARs). These receptors are known to be concentrated within the postsynaptic density (PSD), an electron dense structure expressed at postsynaptic site (Sheng and Hoogenraad, 2007). Kainate-type glutamate receptors (KARs) are the least characterized ionotropic glutamate receptors as to their molecular identities of the receptor complex, the detailed subcelluler localization, and their dynamics and the trafficking mechanism (Contractor et al., 2011). KARs are assembled from combinations of five subunits, GluK1-5, and show heterogenous region-specific distribution in the brain (Monaghan & Cotman, 1982, Wisden and Seeburg, 1993). In the hippocampus, KARs are most abundantly expressed in the stratum lucidum of CA3 region where mossy fibers terminate (Straub et al., 2011). Presynaptic as well as postsynaptic actions of KARs have been demonstrated so far. Application of low concentration of kainate, an agonist of KARs, regulates transmitter release in a biphasic fashion at mossy fiber-CA3 synapse (Kamiya and Ozawa, 2000; Lauri et al.,

2001; Schmitz et al., 2001). In addition, KARs-mediated slow postsynaptic currents are observed under the blockade of AMPARs at mossy fiber-CA3 synapse (Castillo et al., 1997; Vignes and Collingridge, 1997). On the other hand, stimulation of associational/commissural fiber-CA3 synapse did not elicit any KARs-mediated responses. Although KARs-mediated postsynaptic currents are relatively smaller than those of AMPARs, it is thought that they contribute to the synaptic summation to a large degree because of its slower kinetics (Sachidhanandam et al., 2009), and therefore critically contributed for the unique roles as "conditional detonator" of the mossy fiber synapse.

In contrast to the case of AMPARs, little is known about mechanisms of synaptic localization of KARs. It has been reported that several molecules directly or indirectly interact with KARs subunits. For instance, PDZ domain-containing proteins GRIP and PICK1 interact with GluK1 and GluK2 (Hirbec et al., 2003). It is also reported that cadherin/ß-catenin complex indirectly interact with GluK2 (Coussen et al., 2002). It should be noted that PSD-95, a major scaffold protein in the PSD, was demonstrated to bind directly to GluK2 and GluK5 in biochemical study (Garcia et al., 1999) and the PSD-95 accelerates the recovery from desensitization of GluK2

(Bowie et al., 2003). Although deletion of PSD-95 reduces synaptic AMPARs (Béïque et al., 2006; Carlisle et al., 2008), the changes in postsynaptic KARs in PSD-95 knockout mice have not been tested so far. In the present study, we examined the issue whether synaptic KARs changed in the complete absence of PSD-95 in the knockout mice.

2. Materials and Methods

2.1 Animals and slice preparation

PSD-95 knockout mice were purchased from the Jackson Laboratory (Bar Harbor, ME, USA, http://jaxmice.jax.org/strain/013099.html, Béïque et al., 2006) and fed in-house. All animals were treated according to the guidelines for the care and use of laboratory animals of Hokkaido University. Hippocampal slices were obtained from wild type mice (littermate) and PSD-95 knockout mice of either sex (p13-p28, number of animals = 42) as described previously (Kamiya, 2012). Briefly, mice were deeply anesthetized with an overdose of ether and decapitated. Then the brains were quickly removed and chilled with ice-cold sucrose-based cutting solution containing the following (in mM): 40 NaCl, 25 NaHCO3, 10 glucose, 150 sucrose, 4 KCl, 1.25 NaH_2PO_4, 0.5 $CaCl_2$ and 7 $MgCl_2$. Transverse hippocampal slices (300 μm thick) were cut using a microslicer (Pro-7, Dosaka-EM, Kyoto, Japan). The slices were kept in an interface-type chamber supplemented with the artificial cerebrospinal fluid (ACSF) containing the following (in mM): 127 NaCl, 1.5 KCl, 1.2 KH_2PO_4, 26 $NaHCO_3$, 2.4 $CaCl_2$, 1.3 $MgSO_4$ saturated with 95% O_2 and 5% CO_2 at room temperature (around 25°C). All

experiments were carried out in double-blind fashion.

2.2 Electrophysiology.

The slices were perfused with ACSF at a rate of 2.0 ml/min and maintained at 24-26°C in a submerged recording chamber. The granule cell layer of dentate gyrus was stimulated every 10 s. To eliminate the GABAergic responses, CA3 neurons were voltage clamped at -67 mV (= E_{Cl}). The junction potential was estimated as -15 mV using pCLAMP 10 software (Molecular Devices, Sunnyvale, CA, USA) to compensate the holding potential. Patch pipettes (3-10 MΩ) were filled with an internal solution containing the following (in mM): 140 K-gluconate, 10 KCl, 0.2 EGTA, 2 MgATP, 10 HEPES, 0.5 lidocaine *N*-ethyl bromide quaternary salt (QX-314), adjusted to pH 7.2. The data were excluded if the series resistance changed >20% of the initial value. For rapid and local application of drugs, a flow pipe connecting to an electromagnetic valve system (ValveBank; Automate Scientific, Berkeley, CA, USA) was placed on the surface of the slices near the recording site as described previously (Kamiya, 2012). An agonist of group II metabotropic glutamate receptor, DCG-IV (1 μM), was used to verify

the selective stimulation of the mossy fiber input (Kamiya et al., 1996).

To examine the changes in postsynaptic KARs, we compared the size of KARs-mediated field EPSPs (fEPSPs) (Rouach et al., 2005) between wild type mice and PSD-95 knockout mice. Repetitive stimulation (3 pulses at 100 Hz, 0.033 Hz) was applied to evoke the measurable size of KARs-mediated slow components. The size of the fiber volley and AMPARs-mediated fEPSPs were evaluated from the 1st response. The size of KARs-mediated fEPSPs was measured as the amplitude of the 3rd fEPSPs in the presence of 30 μM GYKI 53655. The size of fEPSPs was compared with the size of the fiber volley to normalize the numbers of stimulated axons. In this set of experiment, the stimulus intensity was adjusted to evoke the fiber volley amplitude about 0.5 mV.

The recording of KARs-mediated miniature EPSC ($mEPSC_{KA}$) was performed at -80 mV, using patch pipettes were filled with an internal solution containing the following (in mM): 150 Cs-gluconate, 8 NaCl, 2 MgATP, 10 HEPES, 0.2 EGTA, and 0.5 QX-314, adjusted to pH 7.2. Bath application of normal ACSF including picrotoxin often elicits the epileptic activity in the CA3 region, where the dense recurrent excitatory network

exists. Therefore, we perfused the Ca^{2+}-free ACSF (equal concentration of Mg^{2+} was replaced for Ca^{2+}) in the bath, and Ca^{2+}-containing normal ACSF including 1 μM tetrodotoxin, 30 μM GYKI 53655, 25 μM D-AP5 and 100 μM picrotoxin was focally applied to the recording site. In the present study, we recorded $mEPSC_{KA}$ for one minute from each cell, and the mean frequency were 8.3 ± 2.4 events/min in wild-type (8 cells, 66 events in total) and 2.7 ± 0.9 events/min in PSD-95 knockout (13 cells, 35 events in total). Similar results of low frequency of $mEPSC_{KA}$ at the wild-type mossy fiber-CA3 synapse have been reported in the previous studies of Neto 1 and Neto 2 knockout mice (Wyeth et al., 2014) and GluK4 overexpressing transgenic mice (Aller et al., 2015). To examine the changes in the release probability from the presynaptic terminals, paired-pulse stimulation was applied at 50 ms interstimulus interval. The strength of the electrical stimulation was set to evoke AMPARs-mediated first EPSC about 100 pA.

Signals were filtered at 1 kHz (except for the recording of $mEPSC_{KA}$ at 600 Hz). The $mEPSC_{KA}$ was analyzed using MiniAnalysis Program 6.0.3 (Synaptosoft, Fort Lee, NJ, USA). An amplitude threshold of 3 pA and a decay time constant longer than 20 ms were used for detection criteria of

mEPSC$_{KA}$.

2.3 Chemicals

QX-314 and GYKI 53655 were purchased from Sigma-Aldrich (St. Louis, MO, USA). ACET (UBP316, Dolman et al., 2007), D-AP5 and DCG-IV were purchased from Tocris Bioscience (Bristol, UK). Tetrodotoxin was purchased from Funakoshi (Tokyo, Japan). All other chemicals were purchased from Wako Pure Chemical Industries (Tokyo, Japan).

2.4 Statistics

Data are expressed as the mean ± SEM, and n represents the number of recording neurons. Statistical analyses for comparison between the two groups (wild-type and knockout mice) were performed by Mann-Whiteney U test, and p-values of < 0.05 were accepted for significance.

3. Results

3.1 Reduced KA/AMPA ratio in PSD-95 knockout mice.

EPSCs at mossy fiber-CA3 synapse consists of fast and slow components (Castillo et al., 1997; Vignes and Collingridge, 1997). Fast components are mediated by AMPAR, since they were abolished by application of selective AMPAR antagonist GYKI 53655. Slow components were shown to be suppressed by further application of AMPAR/KAR blocker CNQX, and therefore supposed to be mediated by KARs. Thus, we examined the consequence of deletion of PSD-95 on postsynaptic KARs at hippocampal mossy fiber synapses.

First, we examined the KA/AMPA ratio for exploring the changes in postsynaptic KARs, since NMDARs-mediated currents were not invariably recorded under the voltage clamp recording at -67 mV in the solution that Mg^{2+} was replaced with Ca^{2+}. The KA/AMPA ratio was calculated as ACET-sensitive KARs-mediated component divided by GYKI 53655-sensitive AMPARs-mediated component of EPSCs. Since KARs-mediated components are small and slow, we analyzed amplitude as well as charge transfer to measure KARs-mediated currents quantitatively. Charge transfer was

calculated as the integral of the area under the synaptic currents. In wild type mice, slow components were observed in the presence of GYKI 53655 (amplitude: to 11.7 ± 0.9% of control, charge transfer: to 27.4 ± 2.5% of control, n = 16, Fig. 1A). These slow components were suppressed by the additional application of 1 μM ACET (amplitude: to 5.3 ± 0.6% of control, charge transfer: to 9.0 ± 1.8% of control, Fig. 1A). This result is consistent with a previous study showing that 2 μM ACET partly suppressed KARs-mediated currents at mossy fiber-CA3 synapse (Pinheiro et al., 2013, but see Dargan et al., 2009). In PSD-95 knockout mice, substantial GYKI-resistant slow components were observed (amplitude: to 8.7 ± 0.7% of control, charge transfer: to 18.9 ± 2.0% of control, n = 8, Fig. 1A), and these slow components were suppressed by ACET (amplitude: to 4.9 ± 0.7% of control, charge transfer: to 8.5 ± 2.7% of control, Fig. 1A). It was notable that the KA/AMPA ratio in PSD-95 knockout mice was significantly smaller than that of wild type mice (amplitude: $p = 0.045$, charge transfer: $p = 0.023$, Fig. 1B). These results suggest that synaptic KARs are reduced in PSD-95 knockout mice. However, the decay time constants of KARs-mediated slow current were not changed significantly (wild type: 65.8 ± 7.8 ms, PSD-95

knockout: 65.0 ± 4.2 ms, $p = 0.83$, Fig. 1B). Therefore, it seems that PSD-95 was not involved in the regulation of the gating of synaptic KARs.

3.2 Reduced KARs-mediated fEPSPs in PSD-95 knockout mice.

Although reduced KA/AMPA ratio may reflect the relative decrease in the postsynaptic KARs, an alternative possibility is that AMPARs at mossy fiber-CA3 synapses may increase in PSD-95 knockout. Then we attempted to evaluate the absolute change of postsynaptic KARs. For this purpose, we examined the input-output relationship by comparing the size of the KARs-mediated fEPSPs with the size of the fiber volley, the compound action potentials of the presynaptic axons. Repetitive stimulation (3 pulses at 100 Hz, 0.033 Hz) was applied to dentate granule cell layer to elicit the measurable size of KARs-mediated component. AMPARs-mediated fEPSPs were evaluated by the size of the first fEPSPs (Fig. 2A), which were abolished by the application of GYKI 53655 (Fig. 2B). The relative size of AMPARs-mediated fEPSPs normalized by the size of the fiber volley in PSD-95 knockout mice was significantly smaller than that of wild type mice (wild type: 0.59 ± 0.06, n = 12, PSD-95 knockout: 0.35 ± 0.05, n = 11, Fig. 2A,

$p = 0.011$). This result is in line with a previous report showing that AMPARs at the Schaffer collateral-CA1 synapse were largely reduced in PSD-95 knockout mice (Béïque et al., 2006). In the presence of GYKI 53655, slow components were observed at the 3rd fEPSPs (Fig. 2B). They were suppressed by the additional application of ACET, therefore, represented the KARs-mediated fEPSPs. The relative size of KARs-mediated fEPSPs normalized by the size of the fiber volley in PSD-95 knockout mice was significantly smaller than that of wild type mice (wild type: 1.00 ± 0.1, PSD-95 knockout: 0.58 ± 0.06, Fig. 2B, $p = 0.0045$). These results strongly suggest that the postsynaptic KARs is reduced in PSD-95 knockout mice.

3.3 Decreased frequency of KARs-mediated miniature EPSCs in PSD-95 knockout mice.

Next, we examined the KARs-mediated miniature EPSCs ($mEPSC_{KA}$), which directly reflects the amount of postsynaptic KARs. Since the occurrence of $mEPSC_{KA}$ was less often, especially in PSD-95 knockout mice, the analysis of cumulative probability distribution was not practically feasible (Wyeth et al., 2014). Thus, we calculated the mean frequency and

amplitude of $mEPSC_{KA}$ of 1 min observation periods. All recordings from the CA3 neurons in wild type mice, mEPSCs were recorded in the presence of tetrodotoxin, GYKI 53655, D-AP5, and picrotoxin (8.3 ± 2.4 events/min, n = 8, Fig. 3A, top traces). These mEPSCs were abolished by additional application of ACET, suggesting to reflect $mEPSC_{KA}$. In PSD-95 knockout mice, however, fewer events were detected (2.7 ± 0.9 events/min, n = 13, Fig. 3A, bottom traces). Notably, 3 of 13 cells did not show any $mEPSC_{KA}$ in PSD-95 knockout mice. The mean frequency of $mEPSC_{KA}$ in PSD-95 knockout mice was significantly reduced (Fig. 3B, $p = 0.034$). However, the mean amplitude of $mEPSC_{KA}$ was not changed (wild type: 9.4 ± 0.6 pA, PSD-95 knockout: 11.6 ± 1.4 pA except for 3 cells, which didn't show any $mEPSC_{KA}$, Fig. 3B, $p = 0.15$). The decay time constants of $mEPSC_{KA}$ were not changed significantly (wild type: 35.9 ± 0.74 ms, PSD-95 knockout: 35.1 ± 1.15 ms, $p = 0.34$). A rather straight forward interpretation of the reduction of the frequency of $mEPSC_{KA}$ without changes in the amplitude could be the reduction of the transmitter release from the presynaptic terminals. To test the effect of the deletion of PSD-95 on transmitter release probability, we examined the change in paired-pulse facilitation characteristic for this synapse. We measured the

paired-pulse ratio of AMPAR-mediated evoked EPSCs at 50 ms interval, and there was no significant difference between wild type and PSD-95 knockout mice (wild type: 3.8 ± 0.4, n = 5, PSD-95 knockout: 3.9 ± 0.3, n = 8, Fig. 4, p = 0.94), as shown in the previous study on CA1 synapses in the same strain of mice (Béïque et al., 2006). Since KAR may not distribute evenly with AMPAR, we also checked if there were any changes paired-pulse ratio of KAR-mediated fEPSPs ($fEPSP_{KA}$). Because the first $fEPSP_{KA}$ in response to three consecutive stimuli were quite small in size (< 0.1 mV in most recordings, Fig.2B), and therefore were difficult to quantify the amplitude of the first responses reliably. Alternatively, we calculated the ratio of the second and the third responses. These values of the facilitation ratio of the third and the second responses were not significantly different between wild-type (3.5 ± 0.4, n = 12) and PSD-95 knockout (3.7 ± 0.6, n= 11; p = 0.34, Fig. 2). Therefore, the probability of transmitter release at the KAR-containing mossy fiber synapse seems to be unaltered in PSD-95 knockout mice.

Another interpretation is that the amplitude of $mEPSC_{KA}$ might fall below the threshold of detection in PSD-95 knockout mice (3 pA in the

present study), since the amplitude of $mEPSC_{KA}$ is quite small (Shimizu et al., 2008). Thus, the reduction of mean frequency of $mEPSC_{KA}$ may not reflect the reduced transmitter release, but reflects the decrease of postsynaptic KARs in some population of synapses. The unaltered decay time constants of $mEPSC_{KA}$ in PSD-95 knockout mice supports the view that PSD-95 does not affect the kinetics of synaptic KARs (Fig. 1). All these results indicate that the synaptic KARs is significantly decreased in PSD-95 knockout mice.

4. Discussion

In this study, we examined the role of PSD-95 in the KARs-mediated component of synaptic transmission in hippocampal mossy fiber-CA3 synapse. For this purpose, we analyzed the KA/AMPA ratio of evoked EPSCs, KAR components of field EPSPs, and the KAR-mediated miniature EPSCs in PSD-95 knockout mice. All the results supported that the synaptic KARs is much reduced than synaptic AMPARs in PSD-95 knockout mice. Thus, PSD-95 has a critical role in regulating the synaptic KARs as well as AMPARs.

Although glutamate receptors distribute also on the extrasynaptic membranes, the vast majority are concentrated within the PSD. PSD is a macromolecular complex composed of a number of molecules interacting with the receptors (Sheng and Hoogenraad, 2007). Among them, PSD-95 is a strong candidate of scaffolding molecules for dense expression of glutamate receptors at the postsynaptic sites. Especially in the case of AMPARs, the depletion of PSD-95 decreases (Béïque et al., 2006; Carlisle et al., 2008) and overexpression of them increases synaptic AMPARs (El-Husseini et al., 2000; Schnell et al., 2002). It was reported that PSD-95 directly binds to GluK2

and GluK5 subunit of KARs, and they are colocalized at the synapses in the cultured hippocampal neuron (Garcia et al., 1999). However, there is no direct evidence regarding the role of PSD-95 in the synaptic KARs in intact synapse. Using PSD-95 knockout mice, we examined whether PSD-95 regulates synaptic KARs at the mossy fiber-CA3 synapses, where the highest amount of KARs are expressed in the brain. First, we compared the relative abundance of KARs over AMPARs by measuring the ratio of the amplitudes of AMPARs and KARs mediated components of the EPSCs. The KAR/AMPA ratio of the mossy fiber EPSCs was decreased in PSD-95 knockout mice (Fig.1). Taking into account that the AMPARs-mediated components of the mossy fiber EPSPs were reduced in PSD-95 knockout mice (Fig. 2A) as in the CA1 synapses (Béïque et al., 2006), it was suggested that KARs are likely to be decreased at the mossy fiber-CA3 synapses. Since KA/AMPA ratio reflects a relative change, we also carried out the two independent experiments to examine the absolute change of postsynaptic KARs. First, we examined the input-output relationship by comparing the size of KARs-mediated fEPSPs with the size of the fiber volley. We found that KARs-mediated fEPSPs was significantly decreased in PSD-95 knockout mice than that in wild type mice,

suggesting the reduction of KARs-mediated component of synaptic transmission. Second, we recorded KARs-mediated miniature EPSCs ($mEPSC_{KA}$). The mean frequency of $mEPSC_{KA}$ decreased in PSD-95 knockout mice while the mean amplitude of $mEPSC_{KA}$ was unaltered. Rather straight forward interpretation of these results is that transmitter release might be reduced in PSD-95 knockout mice. However, it is not likely because the paired-pulse ratio was unchanged. Although, we should take into consideration the difference between mEPSC and evoked EPSC, it was reported that the probabilities for mEPSC and evoked EPSC were correlated (Prange and Murphy, 1999). Therefore, the probability of transmitter release might be unchanged in PSD-95 knockout mice. In the previous study, it was also reported that the mean amplitude of $mEPSC_{AMPA}$ was unchanged, but mean frequency was reduced without change in the paired-pulse ratio in PSD-95 knockout mice at Schaffer collateral-CA1 synapses (Béïque et al., 2006). The analysis of the AMPAR sensitivity in single spines using focal uncaging of glutamate revealed the heterogeneous reduction of AMPARs among the CA1 synapses. A subset of synapses showed a deficit of AMPARs-mediated current without changes in the spine volume (Béïque et

al., 2006). They also revealed that AMPAR lacking silent synapses were found on morphologically mature spines at Schaffer collateral-CA1 synapses. If the reduction of KARs at mossy fiber-CA3 synapse is restricted to a subset of synapses as shown in AMPARs at Schaffer collateral-CA1 synapse, the mean frequency of $mEPSC_{KA}$ might reduce without changes in the mean amplitude. It should be noted the amplitude of $mEPSC_{KA}$ is much smaller than that of $mEPSC_{AMPA}$. Therefore, smaller population $mEPSC_{KA}$ cannot be measured using our criteria of detection (threshold of 3 pA). If the amplitude of $mEPSC_{KA}$ were reduced in PSD-95, it could result in the reduction of frequency rather than of amplitude. Taken together, all these results are in consistent with the notion that postsynaptic KARs are reduced in PSD-95 knockout mice. Further studies are needed to show the variation of the reduction of KARs among synapses, using focal uncaging experiments or quantitative immune-electron microscopic study of KAR subunits.

Carta et al. (2013) showed that phosphorylation of GluK5 by CaMKII diminished the binding between GluK5 and PSD-95, and extrasynaptic KARs were increased compensatory. Recently, it was also reported that KARs-mediated synaptic transmission was increased by overexpression of

GluK4, and exogenous GluK4 is colocalized with endogenous PSD-95 at mossy fiber-CA3 synapses (Aller et al., 2015). Our results support the view that KARs are trapped by PSD-95 in the PSD.

In the present study, KARs-mediated slow component of EPSCs was observed in PSD-95 knockout mice, suggesting that a majority of KARs still remains within the PSD in the complete absence of PSD-95. Although PSD-95 is a major scaffold protein within the PSD, other molecules also have been shown to interact with KARs. It is reported that SAP102 is upregulated and compensates for AMPARs-mediated current in PSD-95 and PSD-93 double knockout mice (Elias et al., 2006). Since SAP102 can bind to GluK2 (Garcia et al., 1999), it is one possibility that SAP102 might compensate for and stabilize KARs within the PSD in PSD-95 knockout mice. Aside from SAP family proteins, other proteins in the PSD can interact with KARs. For instance, PDZ domain-containing proteins GRIP and PICK1 interact with KARs (Hirbec et al., 2003). When the interaction of these proteins with KARs is disrupted, KARs-mediated currents are reduced at mossy fiber-CA3 synapse. Interestingly, some differences in the roles of PDZ-interacting proteins, such as GRIP (glutamate receptor interacting protein), in

regulating synaptic AMPAR at CA1 synapse (Daw et al., 2000) and synaptic KAR at mossy fiber-CA3 synapse have been demonstrated (Hirbec et al., 2003). Since the residual components of synaptic KAR as well as AMPAR in PSD-95 knockout mice are supposed to be mediated by KAR- or AMPAR-interacting GRIP or other PDZ proteins such as PICK1, differential effects of PSD95 knockout on synaptic KAR and AMPAR may be interpreted by differences in regulation of AMPAR and KAR by GRIP or the related molecules.

It was also reported that cell-cell adhesion molecules, cadherin/β-catenin complex, indirectly interact with KARs, and stabilize them at the border of PSD (Coussen et al., 2002). The localization of KAR at the border of PSD in the PSD-95 knockout may result in the smaller synaptic KAR responses than AMPAR responses, since the border of PSD is slightly away from the presynaptic release sites of glutamate.

An auxiliary subunit of KARs neuropilin and tolloid-like 1 (Neto1) is abundantly expressed in the stratum lucidum of CA3 region (Michishita et al., 2003; Straub et al., 2011) and immunohistochemistry revealed that the deletion of Neto1 reduced the postsynaptic KARs by half at mossy fiber-CA3

synapse (Wyeth et al., 2014). Therefore, these other molecules might compensate for PSD-95 to maintaining the KARs-mediated currents. In the present study, there was no difference in the decay time course of KARs-mediated components between wild type mice and PSD-95 knockout mice. However, the decay time course of KARs-mediated current was much faster in Neto1 knockout mice than that of wild type mice (Straub et al., 2011). Therefore, PSD-95 regulates the synaptic KARs but not modulate the gating of KARs, in sharp contrast to Neto1.

5. Conclusion

In this study, we demonstrated that synaptic KARs as well as AMPARs were significantly reduced without apparent changes in their time courses in PSD-95 knockout mice. Therefore, PSD-95 has a critical role not only synaptic AMPARs, but also for synaptic KARs at the hippocampal mossy fiber synapses.

Acknowledgements

This work was supported by JSPS KAKENHI grant numbers 241035 to ES, 2430014 to HK.

Abbreviations

AMPARs, AMPA receptors; fEPSPs, field EPSPs; KARs, Kainate receptors; $mEPSC_{KA}$, kainate receptor-mediated miniature EPSC; PSD, postsynaptic density.

References

Aller, M.I., Pecoraro, V., Paternain, A.V., Canals, S., Lerma, J., 2015. Increased Dosage of High-Affinity Kainate Receptor Gene grik4 Alters Synaptic Transmission and Reproduces Autism Spectrum Disorders Features. J. Neurosci., 35, 13619-13628.

Béïque, J. C., Lin, D. T., Kang, M. G., Aizawa, H., Takamiya, K., Huganir, R. L., 2006. Synapse-specific regulation of AMPA receptor function by PSD-95. Proc. Natl. Acad. Sci. USA, 103, 19535-19540.

Bowie, D., Garcia, E. P., Marshall, J., Traynelis, S. F., Lange, G. D., 2003. Allosteric regulation and spatial distribution of kainate receptors bound to ancillary proteins. J. Physiol. (Lond), 547, 373-385.

Carlisle, H. J., Fink, A. E., Grant, S. G., O'Dell, T. J., 2008. Opposing effects of PSD-93 and PSD-95 on long-term potentiation and spike timing-dependent plasticity. J. Physiol. (Lond), 586, 5885-5900.

Carta, M., Opazo, P., Veran, J., Athané, A., Choquet, D., Coussen, F., Mulle, C., 2013. CaMKII-dependent phosphorylation of GluK5 mediates plasticity of kainate receptors. EMBO J., 32, 496-510.

Castillo, P. E., Malenka, R. C., Nicoll, R. A. 1997. Kainate receptors mediate

a slow postsynaptic current in hippocampal CA3 neurons. Nature, 388, 182-186.

Contractor, A., Mulle, C., Swanson, G. T., 2011. Kainate receptors coming of age: milestones of two decades of research. Trends. Neurosci., 34, 154-163.

Coussen, F., Normand, E., Marchal, C., Costet, P., Choquet, D., Lambert, M., Mège, R. M., Mulle, C., 2002. Recruitment of the kainate receptor subunit glutamate receptor 6 by cadherin/catenin complexes. J. Neurosci., 22, 6426-6436.

Dargan, S. L., Clarke, V. R., Alushin, G. M., Sherwood, J. L., Nisticò, R., Bortolotto, Z. A., Ogden, A. M., Bleakman, D., Doherty, A. J., Lodge, D., Mayer, M. L., Fitzjohn, S. M., Jane, D. E., Collingridge, G. L., 2009. ACET is a highly potent and specific kainate receptor antagonist: characterisation and effects on hippocampal mossy fibre function. Neuropharmacology, 56, 121-130.

Daw, M. I., Chittajallu, R., Bortolotto, Z. A., Dev, K. K., Duprat, F., Henley, J. M., Collingridge, G. L., Isaac, J. T. 2000. PDZ proteins interacting with C-terminal GluR2/3 are involved in a PKC-dependent regulation of AMPA receptors at hippocampal synapses. Neuron, 28, 873-886.

Dolman, N.P., More, J.C., Alt, A., Knauss, J. L., Pentikäinen, O. T., Glasser, C. R., Bleakman, D., Mayer, M. L., Collingridge, G. L., Jane, D. E., 2007. Synthesis and pharmacological characterization of N3-substituted willardiine derivatives: role of the substituent at the 5-position of the uracil ring in the development of highly potent and selective GLUK5 kainate receptor antagonists. J. Med. Chem., 50, 1558-1570.

Elias, G. M., Funke, L., Stein, V., Grant, S. G., Bredt, D. S., Nicoll, R. A., 2006. Synapse-specific and developmentally regulated targeting of AMPA receptors by a family of MAGUK scaffolding proteins. Neuron, 52, 307-320.

El-Husseini, A. E., Schnell, E., Chetkovich, D. M., Nicoll, R. A., Bredt, D. S., 2000. PSD-95 involvement in maturation of excitatory synapses. Science, 290, 1364-1368.

Garcia, E. P., Mehta, S., Blair, L. A., Wells, D. G., Shang, J., Fukushima, T., Fallon, J. R., Garner, C. C., Marshall, J., 1998. SAP90 binds and clusters kainate receptors causing incomplete desensitization. Neuron, 21, 727-739.

Hirbec, H., Francis, J. C., Lauri, S. E., Braithwaite, S. P., Coussen, F., Mulle,

C., Dev, K. K., Coutinho, V., Meyer, G., Isaac, J. T., Collingridge, G. L., Henley, J. M., 2003. Rapid and differential regulation of AMPA and kainate receptors at hippocampal mossy fibre synapses by PICK1 and GRIP. Neuron, 37, 625-638.

Kamiya, H., 2012. Photochemical inactivation analysis of temporal dynamics of postsynaptic native AMPA receptors in hippocampal slices. J. Neurosci., 32, 6517-6524.

Kamiya, H., Ozawa, S., 2000. Kainate receptor-mediated presynaptic inhibition at the mouse hippocampal mossy fibre synapse. J. Physiol. (Lond), 523, 653-665.

Kamiya, H., Shinozaki, H., Yamamoto, C., 1996. Activation of metabotropic glutamate receptor type 2/3 suppresses transmission at rat hippocampal mossy fibre synapses. J. Physiol. (Lond), 493, 447-455.

Lauri, S. E., Bortolotto, Z. A., Bleakman, D., Ornstein, P. L., Lodge, D., Isaac, J. T., Collingridge, G. L., 2001. A critical role of a facilitatory presynaptic kainate receptor in mossy LTP. Neuron, 32, 697-709.

Michishita, M., Ikeda, T., Nakashiba, T., Ogawa, M., Tashiro, K., Honjo, T., Doi, K., Itohara, S., Endo, S., 2003. A novel gene, Btcl1, encoding CUB and

LDLa domains is expressed in restricted areas of mouse brain. Biochem. Biophys. Res. Commun. 306, 680-686.

Monaghan, D. T., Cotman, C. W., 1982. The distribution of [3H]kainic acid binding sites in rat CNS as determined by autoradiography. Brain. Res., 252, 91-100.

Pinheiro, P. S., Lanore, F., Veran, J., Artinian, J., Blanchet, C., Crépel, V., Perrais, D., Mulle, C., 2013. Selective block of postsynaptic kainate receptors reveals their function at hippocampal mossy fiber synapses. Cereb. Cortex, 23, 323-331.

Prange, O., Murphy, T. H., 1999. Correlation of miniature synaptic activity and evoked release probability in cultures of cortical neurons. J. Neurosci., 19, 6427-6438.

Rouach, N., Byrd, K., Petralia, R. S., Elias, G. M., Adesnik, H., Tomita, S., Karimzadegan, S., Kealey, C., Bredt, D. S., Nicoll, R. A., 2005. TARP gamma-8 controls hippocampal AMPA receptor number, distribution and synaptic plasticity. Nat. Neurosci., 8, 1525-1533.

Sachidhanandam, S., Blanchet, C., Jeantet, Y., Cho, Y. H., Mulle, C., 2009. Kainate receptors act as conditional amplifiers of spike transmission at

hippocampal mossy fiber synapses. J. Neurosci., 29, 5000-5008.

Schmitz, D., Mellor, J., Nicoll, R. A., 2001. Presynaptic kainate receptor mediation of frequency facilitation at hippocampal mossy fiber synapses. Science, 291, 1972-1976.

Schnell, E., Sizemore, M., Karimzadegan, S., Chen, L., Bredt, D. S., Nicoll, R. A., 2002. Direct interactions between PSD-95 and stargazin control synaptic AMPA receptor number. Proc. Natl. Acad. Sci. USA, 99, 13902-13907.

Sheng, M., Hoogenraad, C. C., 2007. The postsynaptic architecture of excitatory synapses: a more quantitative view. Annu. Rev. Biochem., 76, 823-847.

Shimizu, H., Fukaya, M., Yamasaki, M., Watanabe, M., Manabe, T., Kamiya, H., 2008. Use-dependent amplification of presynaptic Ca^{2+} signaling by axonal ryanodine receptors at the hippocampal mossy fiber synapse. Proc. Natl. Acad. Sci. USA, 105, 11998-12003.

Straub, C., Hunt, D. L., Yamasaki, M., Kim, K. S., Watanabe, M., Castillo, P. E., Tomita, S., 2011. Distinct functions of kainate receptors in the brain are determined by the auxiliary subunit Neto1. Nat. Neurosci., 14, 866-873.

Vignes, M., Collingridge, G. L., 1997. The synaptic activation of kainate receptors. Nature, 388, 179-182.

Wisden, W., Seeburg, P. H., 1993. A complex mosaic of high-affinity kainate receptors in rat brain. J. Neurosci., 13, 3582-3598.

Wyeth, M. S., Pelkey, K. A., Petralia, R. S., Salter, M. W., McInnes, R. R., McBain, C. J., 2014. Neto auxiliary protein interactions regulate kainate and NMDA receptor subunit localization at mossy fiber-CA3 pyramidal cell synapses. J. Neurosci., 34, 622-628.

Figure Legends.

Figure 1. The KA/AMPA ratio is reduced in PSD-95 knockout mice. (A) Slow currents were observed in the presence of 30 μM GYKI 53655 in wild type mice and further application of 1 μM ACET suppressed these slow currents (left). In PSD-95 knockout mice, GYKI-resistant and ACET-sensitive slow components were much reduced (right). Traces of AMPAR-mediated current (control) and KAR-mediated current (GYKI) are peak scaled for comparison of the time courses. (B) Summary data of KA/AMPA ratio of amplitude and charge transfer, and decay time constant of KAR-mediated current in wild type (n = 16) and PSD-95 knockout mice (n = 8). *$p < 0.05$

Figure 2. AMPARs and KARs mediated fEPSPs are reduced in PSD-95 knockout mice. (A) Traces in which the fiber volleys (arrowheads) are scaled for comparison of the input-output relationships of AMPARs-mediated fEPSPs ($fEPSP_{AMPAR}$, thin arrows, left). The right panel shows summary data of $fEPSP_{AMPAR}$/fiber volley (FV) ratio in wild type (n = 12) and PSD-95 knockout mice (n = 11). (B) Top: KARs-mediated fEPSPs ($fEPSP_{KAR}$) evoked

by the repetitive stimulation (3 pulses at 100 Hz, 0.033 Hz) in the presence of 30 μM GYKI 53655 in wild type (left) and in PSD-95 knockout mice (right). Bottom: Traces of the $fEPSP_{KAR}$ (thick arrow) were superimposed (left). The right panel shows summary data of $fEPSP_{KAR}$/fiber volley (FV) ratio. **$p < 0.01$, *$p < 0.05$

Figure 3. The mean frequency of KARs-mediated mEPSCs is reduced in PSD-95 knockout mice. (A) KARs-mediated miniature EPSCs ($mEPSC_{KA}$) were recorded in the presence of tetrodotoxin (1 μM), GYKI 53655 (30 μM), D-AP5 (25 μM) and picrotoxin (100 μM). Representative traces show $mEPSC_{KA}$ in wild type (upper), and in PSD-95 knockout mice (bottom). (B) Summary data of the mean frequency (upper, left), the mean amplitude (upper, right), and the decay time constant of $mEPSC_{KA}$ (bottom) in wild type ($n = 8$) and PSD-95 knockout mice ($n = 13$).

Figure 4. The probability of transmitter release is unchanged in PSD-95 knockout mice. (A) AMPAR-mediated EPSCs was evoked by paired stimuli with 50 ms interval in wild type (left) and PSD-95 knockout mice (right). (B)

Summary graph of the paired-pulse ratio in wild type (n = 5) and PSD-95 knockout mice (n = 8). *p < 0.05

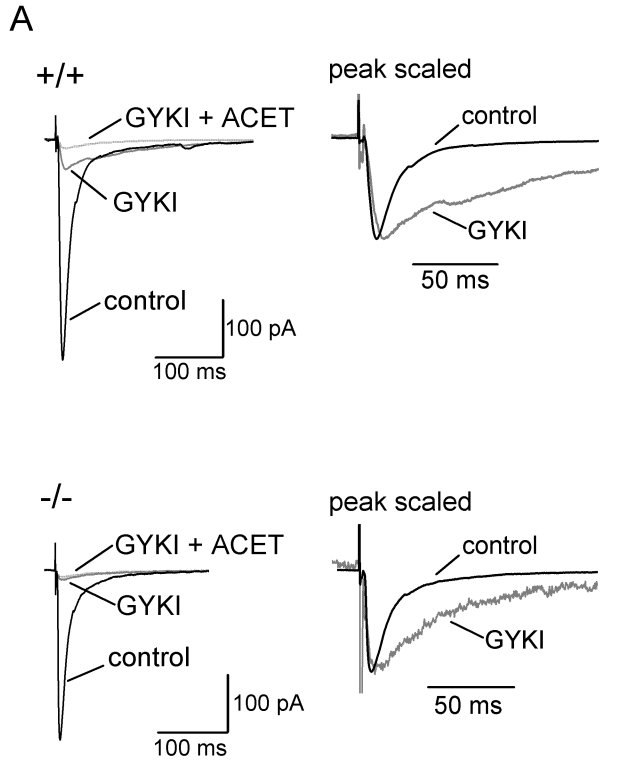
A
+/+
GYKI + ACET
GYKI
control
100 pA
100 ms
peak scaled
control
GYKI
50 ms
-/-
GYKI + ACET
GYKI
control
100 pA
100 ms
peak scaled
control
GYKI
50 ms
B
Amplitude (%)
16
14
12
10
8
6
4
2
0
*
+/+
-/-
Charge transfer (%)
40
30
20
10
0
*
+/+
-/-
Decay time constant (ms)
80
60
40
20
0
n.s.
+/+
-/-

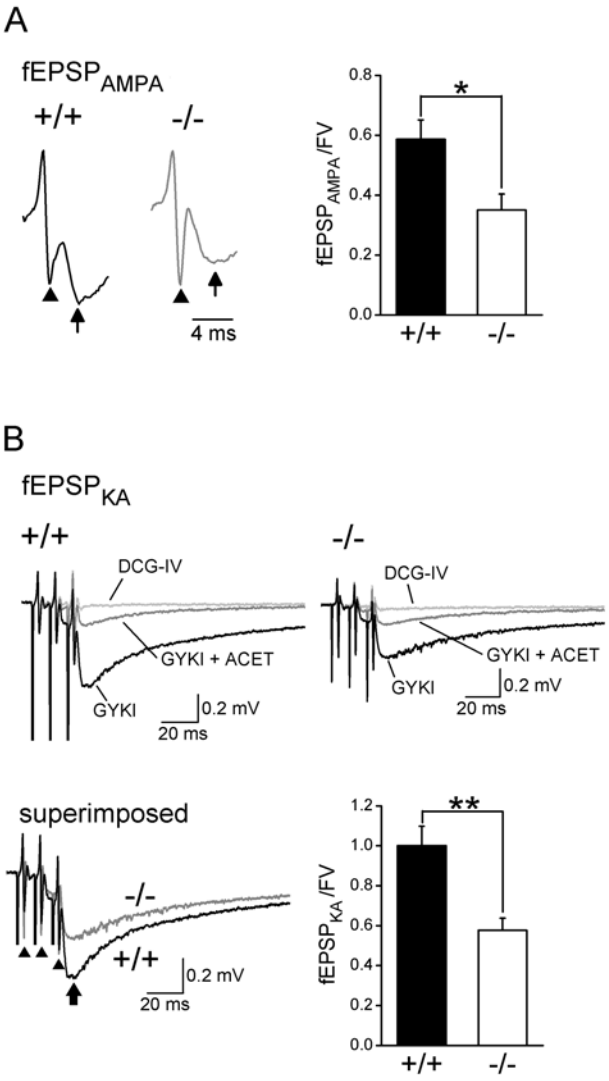
A
fEPSP$_{AMPA}$
+/+
-/-
4 ms
fEPSP$_{AMPA}$/FV
0.8
0.6
0.4
0.2
0.0
*
+/+
-/-
B
fEPSP$_{KA}$
+/+
-/-
DCG-IV
GYKI + ACET
GYKI
0.2 mV
20 ms
superimposed
-/-
+/+
0.2 mV
20 ms
fEPSP$_{KA}$/FV
1.2
1.0
0.8
0.6
0.4
0.2
0.0
**
+/+
-/-

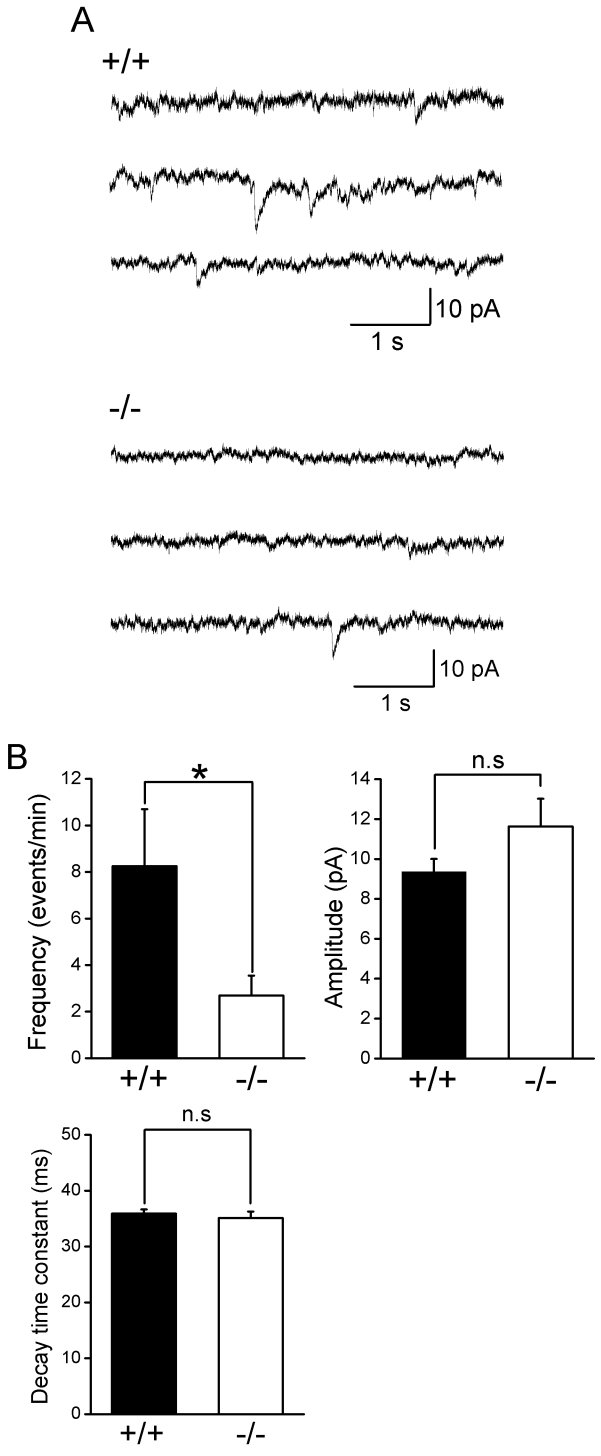
A
+/+
10 pA
1 s
-/-
10 pA
1 s
B
Frequency (events/min)
*
+/+
-/-
Amplitude (pA)
n.s
+/+
-/-
Decay time constant (ms)
n.s
+/+
-/-

Fig. 4 Suzuki, E. & Kamiya, H.